Biophysical Journal Volume 86 February 2004 1002–1011

Response of Equatorial X-Ray Reflections and Stiffness to Altered Sarcomere Length and Myofilament Lattice Spacing in Relaxed Skinned Cardiac Muscle

Donald A. Martyn,* Bishow B. Adhikari,* Michael Regnier,* Jin Gu,† Sengen Xu,† and Leepo C. Yu†

*Department of Bioengineering, University of Washington, Seattle, Washington 98195; and †National Institute of Arthritis, Musculoskeletal and Skin Diseases, National Institutes of Health, Department of Health and Human Services, Bethesda, Maryland 20892

ABSTRACT Low angle x-ray diffraction measurements of myofilament lattice spacing ($D_{1,0}$) and equatorial reflection intensity ratio ($I_{1,1}/I_{1,0}$) were made in relaxed skinned cardiac trabeculae from rats. We tested the hypothesis that the degree of weak cross-bridge (Xbr) binding, which has been shown to be obligatory for force generation in skeletal muscle, is modulated by changes in lattice spacing in skinned cardiac muscle. Altered weak Xbr binding was detected both by changes in $I_{1,1}/I_{1,0}$ and by measurements of chord stiffness (chord K). Both measurements showed that, similar to skeletal muscle, the probability of weak Xbr binding at 170-mM ionic strength was significantly enhanced by lowering temperature to 5°C. The effects of lattice spacing on weak Xbr binding were therefore determined under these conditions. Changes in $D_{1,0}$, $I_{1,1}/I_{1,0}$, and chord K by osmotic compression with dextran T500 were determined at sarcomere lengths (SL) of 2.0 and 2.35 μm. At each SL increasing [dextran] caused $D_{1,0}$ to decrease and both $I_{1,1}/I_{1,0}$ and chord K to increase, indicating increased weak Xbr binding. The results suggest that in intact cardiac muscle increasing SL and decreasing lattice spacing could lead to increased force by increasing the probability of initial weak Xbr binding.

INTRODUCTION

Thin filament activation in cardiac muscle is dependent on 1), Ca^{2+}-binding to cardiac troponin releasing tropomyosin from an inhibitory position on thin filaments, 2), a subsequent effect of actomyosin cross-bridges (Xbr) to enhance the affinity of cardiac troponin for Ca^{2+}, and 3), a direct effect of strong Xbr binding on the state or position of tropomyosin on the thin filament surface (Gordon et al., 2000b). Furthermore, the decrease in Ca^{2+}-sensitivity of force at short sarcomere length (SL) is thought to be based on increased myofilament separation (Fuchs, 2002; Gordon et al., 2000a), with a resultant decrease in the probability of strong Xbr interaction and force generation (McDonald et al., 1997). This length-dependent shift in force Ca^{2+}-sensitivity provides the main basis for the steep relation between filling pressure and myocardial force generation in the intact heart (the Frank-Starling relation). However, changes in SL or lattice spacing could modulate Xbr binding and force generation by at least one other mechanism. In skinned skeletal fibers ''weak'' Xbr binding with rapid association/dissociation kinetics for binding the N-terminus of actin is an obligatory first step on the path to force generation (Brenner et al., 1996a, 1991). Thus, decreasing SL and the corresponding increase in lattice spacing could affect force by modulating the probability of weak Xbr binding to the thin filaments, with little or no direct effect on transitions between weak and strong binding Xbr states. This possibility is supported by the observations that lowering ionic strength (μ), a condition that enhances weak Xbr binding in skinned skeletal fibers (Brenner et al., 1984), causes a decrease in the SL dependence of force-[Ca^{2+}] relations in skinned cardiac muscle (Fuchs and Smith, 2001; Smith and Fuchs, 1999). These results were interpreted in terms of the three state model of thin filament activation (Head et al., 1995; McKillop and Geeves, 1993), where lowered μ could shift the equilibrium between ''blocked'' and ''closed'' thin filament states toward the ''closed state,'' to which Xbr's bind weakly in the absence of activating Ca^{2+} (Head et al., 1995). Therefore, if the properties of weak binding Xbr in cardiac muscle are similar to skeletal muscle, changes in either SL or lattice spacing could alter strong Xbr binding in the presence of Ca^{2+} by modulating the probability of prior Ca^{2+}-insensitive obligatory weak binding (Brenner et al., 1991; Kraft et al., 1999, 1992). If this hypothesis is true, increasing SL or decreasing lattice spacing should cause increased weak Xbr binding in the absence of Ca^{2+} that can be measured by structural and mechanical studies.

At higher temperatures and μ, weakly bound Xbr's with rapid binding/dissociation kinetics make up a small portion of the total population in skeletal fibers, making them difficult to detect (Brenner et al., 1986; Schoenberg et al., 1988). Conditions that enhance weak Xbr binding are lowered μ (Brenner et al., 1984) and lowered temperature (Head et al., 1995). In skinned skeletal fibers lowered temperature favors weak Xbr binding in the absence of Ca^{2+} by favoring the occupancy of the M·ATP state, which is disordered with respect to the thick filament surface, over the more ordered MADP·Pi state (Xu et al. 1999, 1997). For these experiments we chose to lower temperature at higher μ in skinned cardiac muscle to establish conditions that favor

---

Submitted July 7, 2003, and accepted for publication October 22, 2003.

Address reprint requests to Donald A. Martyn, PhD, Dept. of Bioengineering, Box 357962, University of Washington, Seattle, WA 98195. Tel.: 206-543-4478; Fax: 206-685-3300; E-mail: dmartyn@u.washington.edu.

0006-3495/04/02/1002/10 $2.00

weak Xbr binding to cardiac thin filaments. Changes in weak Xbr binding were monitored by low angle x-ray diffraction and corresponding measurements of chord stiffness (chord *K*) when SL was varied (with accompanying changes in lattice spacing) or when SL was constant, and lattice spacing varied independently by osmotic compression with dextran T500.

We found that lowering μ and decreasing temperature at 170-mM μ resulted in an increase in $I_{1,1}/I_{1,0}$ and chord *K* that mimic similar results from skinned skeletal muscle that have been attributed to weak binding of Xbr's to thin filaments. Furthermore, decreased lattice spacing by osmotic compression enhanced both the $I_{1,1}/I_{1,0}$ ratio and attachment measured by chord stiffness at 5°C. The results support the hypothesis that a direct effect of changes of lattice spacing or SL on the probability of weak Xbr binding may contribute to the molecular mechanism of the Frank-Starling relation in cardiac muscle.

METHODS

Preparation

Male Sprague-Dawley rats (150–250 gm) were anesthetized with an intraperitoneal injection of pentobarbital (50 mg/kg) and their hearts removed rapidly and placed in oxygenated, physiological salt solution. Small trabeculae (100–200-μm diameter, 1–2-mm length) were dissected from the right ventricle and their surface membranes rendered permeable to bathing solution constituents by exposing them for at least 30 min at room temperature to a solution containing (in mM): 100 KCl, 9.0 $MgCl_2$, 4.0 MgATP, 5.0 K_2EGTA (ethylene glycol-bis-(β-aminoethylether)-*N*,*N*,*N*′,*N*′-tetraacetic acid), 10 MOPS (3-(*n*-morpholino) propane sulfonic acid), 1% nonionic detergent Triton X-100, pH 7.0, and 50% v/v glycerol. The skinned trabeculae were stored in the same solution without Triton X-100 at −20°C and used for experiments within 1 week. Experimental temperature was between 5 and 25°C, and ion strength was 170 mM.

Solutions

Solution composition was determined according to an iterative computer program that calculates the equilibrium concentration of ligands and ions based on published affinity constants. Proprionate was the major anion. Relaxing solutions contained (in mM): 80 MOPS, 15 EGTA; 1 Mg^{2+}; 3 MgATP; 38 Na^+; 95 K^+; 20 creatine phosphate (CP); and 20 units/ml creatine phosphokinase (CPK), pH 7.0. Rigor solutions contained no MgATP, CP, or CPK. For experiments at low μ (50 mM) solutions contained Imidazole 10, $MgCl_2$ 2, EGTA 2, MgATP 2, CP 10, K proprionate 13, DTT 5, pH 7.0.

Lattice spacing was varied, independent of SL changes, by adding dextran T500 (0–5% (w/v)) to the bathing solutions. After exposure to dextran, the preparation was bathed in relaxing solution with no Dextran, to test for reversibility of changes in lattice dimension.

Mechanical measurements

A detailed description of our mechanical apparatus can be found in (Martyn and Chase, 1995). Chord stiffness (chord *K*) was determined using low amplitude ramp stretches of 0.5% muscle length (ML) at varying rates and monitoring the resulting increase of force during the stretches. The maximal stiffness values were limited by the maximal rate of stretch (ML sec^{-1}) of the motor used to control fiber length (Cambridge Technology Model 300, Watertown, MA); −3db amplitude response 2.4 kHz) and the frequency response of the force transducer (Cambridge Technology Model 400A; resonant frequency 2.2 kHz). Sarcomere length was determined by 633 nm He-Ne laser illumination of the preparation and monitoring the position of the first order diffraction maximum (Chase et al., 1994).

During chord *K* measurements data were filtered to prevent frequency aliasing and acquired at rate that was dependent on the rate of stretch and digitized at 12-bit resolution for analysis with customer software. Statistical analysis was performed using Excel (Microsoft, Redmond, WA). Student's *t*-test was used to compare the means of data.

Low angle x-ray diffraction

X-ray diffraction measurements were done at the high intensity x-ray source at the x-ray Beam Line X27C at National Synchrotron Light Source, Brookhaven National Laboratory, Upton, NY. Chemically skinned right ventricular trabeculae were placed in an upright chamber in which solutions can be exchanged and the preparation exposed to a high intensity synchotron x-ray source. The chamber volume was 1 ml and solution was continuously stirred with a perfusion pump. The optics of Beam X27C uses a double-multilayer (silicon/tungsten) monochronometer. A three pinhole system is used for beam collimation, and the beam diameter is ~400 μm at the preparation. A MAR CCD detector (0.08 × 0.08-mm pixel size) was used for collecting x-ray data. To minimize preparation damage due to x-ray exposure the entire chamber was translated along the fiber axis so that most of the length of the trabecuale was interrogated by the beam. Total exposure time was limited to 4 min for each preparation.

Equatorial intensity from both sides of the meridian of the equatorial x-ray pattern was summed, and the 2-dimensional [1,1] and [1,0] intensity profiles were scanned and integrated. Integrated intensities and spacings of the equatorial diffraction peaks were determined using Peak Fit (SPSS, Chicago, IL).

RESULTS

Representative intensity profiles versus lattice spacing (Å) of the equatorial regions of the low angle x-ray diffraction patterns from a single skinned cardiac trabeculae from rat are shown in Fig. 1. SL was 2.35 μm. The major integrated peaks attributed to [1,0] and [1,1] reflections on the equator are indicated. The [1,1] and [1,0] reflections result from scattering in the lattice planes containing both thick and thin filaments, and only thick filaments, respectively (Squire, 1981). The profiles were obtained from a single preparation and have been displaced vertically for clarity. Profiles were obtained at 25°C and 170-mM μ (*trace 1*), 5°C and 170-mM μ (*trace 2*), and 5°C and 50-mM μ (*trace 3*). The original x-ray patterns corresponding to each intensity profile are shown in the inset. The data were analyzed by fitting the intensity scans with the program Peak Fit for baseline subtraction and determination of the positions of the centroids of the peaks and the values of the integrated intensities under each peak. The lower panel illustrates the residuals of the fit to the corresponding intensity profiles. $D_{1,0}$ (the spacing between the [1,0] planes of the filament lattice) is taken as a measure of lattice dimension and changes in the $I_{1,1}/I_{1,0}$ ratio as a measure of mass redistribution from the region of thick to thin filaments (Malinchik and Yu, 1995; Yu, 1989).

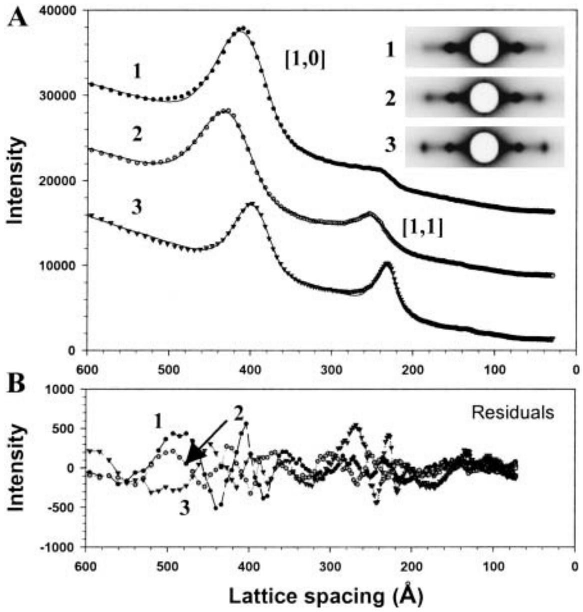

FIGURE 1 (*A*) Representative intensity profiles versus lattice spacing (Å) of the equatorial regions of the low angle x-ray diffraction patterns from a skinned cardiac trabeculae are shown. The dominant integrated peaks attributed to [1,0] and [1,1] reflections on the equator are shown. The profiles were obtained from a single preparation and traces 2 and 3 have been displaced 500 and 1000 units vertically, respectively, for clarity. Profiles were obtained at 25°C and 170-mM μ (*trace 1*), 5°C and 170-mM μ (*trace 2*), and 5°C and 50-mM μ (*trace 3*). Data were analyzed by fitting the intensity scans with the program Peak Fit to determine the positions of the centroids of the peaks and the values of the integrated intensities of each peak. The residuals to the fits of traces 1–3 are shown in *B*.

Effects of temperature on the equatorial intensity ratio and chord stiffness

Studies in skinned skeletal muscle fibers indicate that weak Xbr binding is enhanced by lowering temperature (Xu et al., 1999) as well as by lowering ionic strength (Brenner et al., 1984). The effects of temperature on $D_{1,0}$ (*A*) and intensity ratio ($I_{1,1}/I_{1,0}$) (*B*) in relaxed skinned cardiac muscle at 170-mM μ and 2.35-μm SL are summarized in Fig. 2. Data (means ± SE) was obtained from seven preparations. Decreasing temperature from 25 to 5°C increased both lattice spacing (*A*) and equatorial intensity ratio (*B*) significantly ($p < 0.05$). Lowering temperature at high μ increases $I_{1,1}/I_{1,0}$ in skeletal fibers but decreases $D_{1,0}$ (Xu et al., 1997). Table 1 compares values of $D_{1,0}$ and $I_{1,1}/I_{1,0}$ obtained at 2.0- and 2.35-μm SL at the temperature extremes from Fig. 2, 25 and 5°C. At both 25 and 5°C, $D_{1,0}$ was greater at 2.0 than 2.35 μm ($p < 0.05$); although $I_{1,1}/I_{1,0}$ were slightly less at shorter SL, the difference was not statistically significant ($p > 0.05$). In skeletal fibers the increase $I_{1,1}/I_{1,0}$ when temperature was lowered at higher μ has been attributed to a redistribution of mass toward thin filaments associated with increasing weak attachment of Xbr's (Xu et al., 1997).

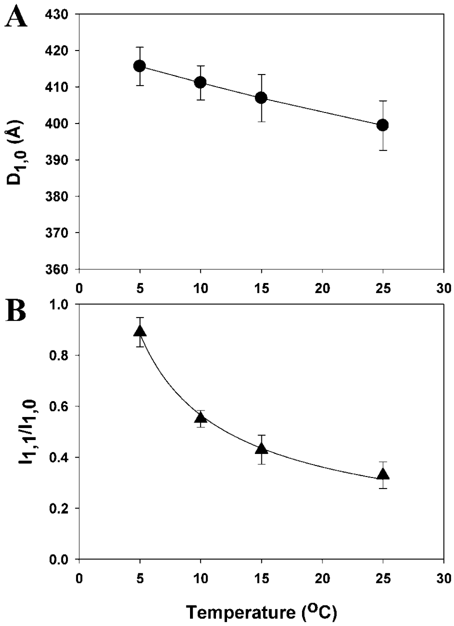

FIGURE 2 The effects of temperature on lattice spacing (*A*) and equatorial intensity ratio (*B*) are illustrated. SL was 2.35 μm and μ was 170 mM. Data (means ± SE) at each temperature was obtained from the same seven preparations.

To estimate the maximal degree of weak Xbr binding in the absence of Ca^{2+}, $D_{1,0}$ and $I_{1,1}/I_{1,0}$ were measured at 5°C and 50-mM μ (SL was 2.35 μm), conditions that favor weak Xbr binding in skeletal fibers (Brenner et al., 1982, 1984). $D_{1,0}$ decreased and $I_{1,1}/I_{1,0}$ increased relative to 5°C and 170-mM μ (Table 1). The decrease of $D_{1,0}$ and increased equatorial intensity ratio at low μ and low temperature in skinned cardiac muscle was similar to skeletal fibers (Xu et al., 1997). The increase of $I_{1,1}/I_{1,0}$ in skinned cardiac muscle was comparable to that observed in skeletal fibers where these changes were attributed to enhanced weak Xbr binding (Brenner et al., 1984; Xu et al., 1997). The value of $I_{1,1}/I_{1,0}$ at 5°C and 170-mM μ (Fig. 2; Table 1) was intermediate between that found at 25°C, 170-mM μ and 5°C, 50-mM μ. This intermediate enhancement of $I_{1,1}/I_{1,0}$ for 5°C and 170-mM μ indicates that the degree of weak Xbr binding under these conditions may be less than maximal compared to 5°C and 50-mM μ, but enhanced relative to higher temperature and higher μ, enabling clear detection of changes in x-ray diffraction and chord *K* measurements. To allow comparison of data obtained under conditions that favor weak Xbr binding to those that favor strong Xbr binding, $D_{1,0}$ and $I_{1,1}/I_{1,0}$ were measured at 2.35-μm SL in rigor, in the absence of Ca^{2+} at 170-mM μ. In rigor $D_{1,0}$ was less than found in relaxed conditions at either 5°C, 50-mM μ or 5°C, 170-mM μ, and the equatorial intensity ratio was much higher (Table 1).

Although increasing $I_{1,1}/I_{1,0}$ ratio suggests a redistribution of mass from thick toward thin filaments (Yu et al., 1985), it does not indicate whether there has been an increased

TABLE 1 Summary of the effects of temperature on $D_{1,0}$ and $I_{1,1}/I_{1,0}$

pCa	n*	SL (μm)	[ATP] (mM)	T (°C)	μ (mM)	$D_{1,0}$ (Å)	$I_{1,1}/I_{1,0}$
~9	15	2.35	5	25	170	388.5 ± 6.5	0.38 ± 0.05
~9	7	2.0	5	25	170	402.7 ± 3.52	0.30 ± 0.04
~9	12	2.35	5	5	170	401.8 ± 3.7	0.85 ± 0.07
~9	6	2.0	5	5	170	416.1 ± 2.83	0.79 ± 0.05
~9 (low μ)	8	2.35	5	5	50	387.2 ± 3.8	1.10 ± 0.08
~9 (rigor)	4	2.35	0	25	170	372 ± 1.84	5.0 ± 0.54

*Number of preparations.

interaction between actin and myosin. To test whether the increase in the $I_{1,1}/I_{1,0}$ ratio as temperature was lowered to 5°C (Fig. 2; Table 1) was associated with enhanced weak Xbr binding, chord K was measured in a parallel set of experiments at 5 and 25°C (170-mM μ) under identical conditions to the x-ray experiments. The combination of chord K (Brenner et al., 1982; Schoenberg, 1988) and x-ray diffraction (Brenner et al., 1984) measurements have been used to detect the presence of weak binding Xbr's in skinned skeletal fibers. Chord K increases at increasing rates of stretch because weak Xbr binding is characterized by a rapid equilibrium between attached and detached states, with faster stretch applying more strain to bound Xbr's (Schoenberg, 1985, 1988). Constant amplitude stretches (+0.15% fiber length) were applied at different rates to relaxed (pCa ~9) skinned trabeculae and the corresponding stiffness (force/stretch amplitude) plotted against the rate of stretch in Fig. 3. For reference chord K in each preparation is expressed as a fraction of the maximal value of stiffness obtained in a maximal Ca^{2+}-activated (pCa 4.5) contraction at 15°C. The top panels illustrate the dependence of chord K on the rate of stretch at 25°C (*solid symbols*) and 5°C (*open symbols*) obtained at 2.0- (*A*) and 2.35-μm (*C*) SL. Panels *B* and *D* illustrate the difference in chord K between 25 and 5°C for the corresponding data in *A* and *C*, respectively. The results in *B* and *D* represent the averages (means ± SE) of the difference in chord K at 5 and 25°C for each rate of stretch. Decreasing temperature resulted in no change of K for slow rates of stretch and caused increased K for faster rates at both SL's. At 2.0-μm SL and the slowest rates of stretch resting K was near zero, whereas at 2.35-μm SL resting tension was 15–20% maximal Ca^{2+}-activated tension and K was

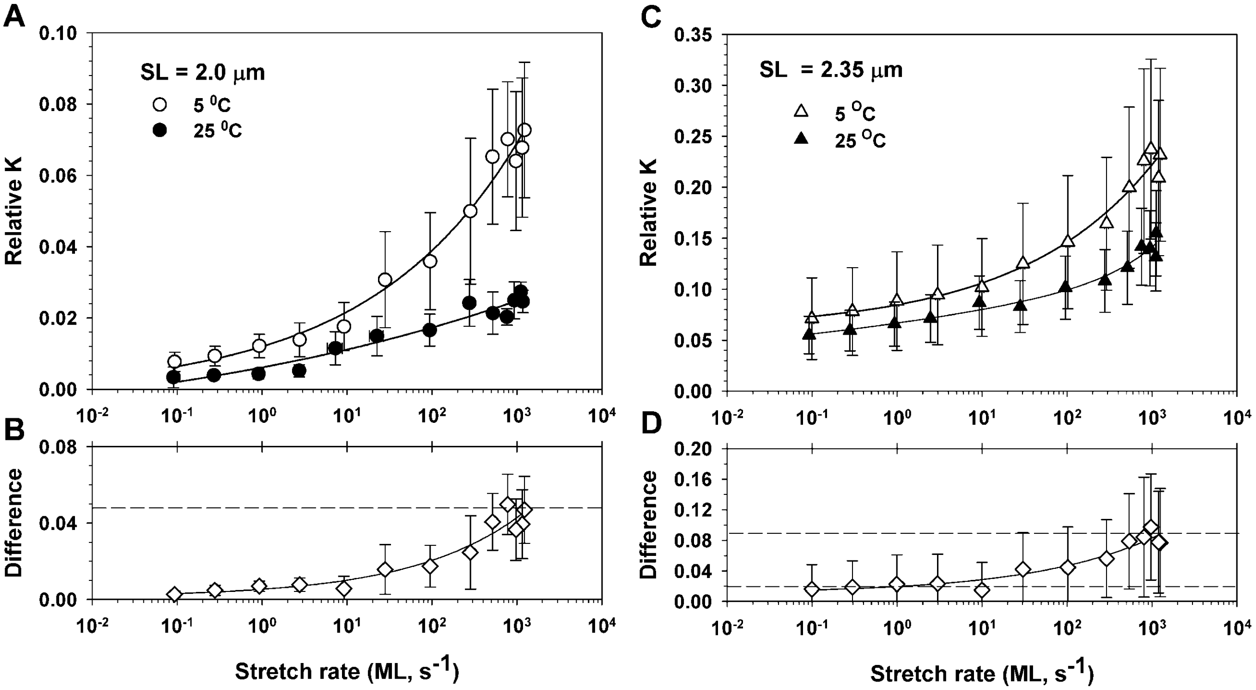

FIGURE 3 Chord stiffness (K) was measured in skinned cardiac preparations under relaxing conditions at 5°C (*open symbols*) and 25°C (*solid symbols*) at 2.0 (*A*) and 2.35 μm (*C*). Constant amplitude stretches (+0.15% fiber length) were applied at different rates to relaxed (pCa ~9) skinned trabeculae and the corresponding stiffness (force/stretch amplitude) plotted against the rate of stretch. *B* and *D* illustrate the difference in chord K for the corresponding data in *A* and *C*, respectively. Data (means ± SE) were obtained from five preparations in *A* and *B* and seven preparations in *C* and *D*. The dotted lines in *B* and *D* are for reference only. For reference, chord K in each preparation is expressed as a fraction of the maximal value of stiffness obtained in a maximal Ca^{2+}-activation (pCa 4.5) contraction at 15°C.

elevated at all rates of stretch (Fig. 3 *C*). Because steady passive force and stiffness are elevated at 2.35-μm SL (Fig. 3, *C* and *D*) some of the increase in chord *K* at 5°C could reflect increased stiffness of passive structures, rather than increased weak Xbr interaction. If this were true the stiffness of passive structures might be expected to increase at all rates of stretch, which was not the case (Fig. 3, *C* and *D*). Chord *K* was unaffected by temperature at the slowest rates of stretch and increased at higher rates, similar to shorter SL where passive force and stiffness were much lower (Fig. 3, *A* and *B*). The absence of an effect of temperature on chord *K* at slower rates of stretch and the similar elevation of chord *K* at higher rates of stretch at 5°C, whether passive force and stiffness were higher or lower, suggests that increased chord *K* at 2.35-μm SL and 5°C probably reflects increased weak Xbr binding and not only increased stiffness of non-Xbr, passive tension bearing structures. The correlation between increased chord *K* at both SL's in Fig. 3 and increased equatorial intensity ratios (Fig. 2; Table 1) indicates that lowering temperature caused enhanced weak Xbr binding to cardiac thin filaments.

Effects of SL and osmotic compression with dextran on lattice spacing and equatorial intensity ratio

To determine if changes in SL and/or lattice spacing modulate the degree of weak Xbr binding in relaxed skinned trabeculae, we measured the SL dependence of $D_{1,0}$ (Fig. 4) and $I_{1,1}/I_{1,0}$ (Fig. 5) under conditions that enhance weak Xbr binding (170 mM, 5°C). $D_{1,0}$ was measured at 2.0- and 2.35-μm SL and varied independent of SL by adding up to 5% dextran T500 to bathing solutions. Data (means ± SE) in Figs. 4 and 5 were obtained from the same six preparations. The solid vertical bar illustrates the change of lattice spacing between 2.0-μm (*top*) and 2.35-μm (*bottom*) SL in intact cardiac trabeculae, as described in Irving et al. (2000). For comparison Table 1 contains $D_{1,0}$ values obtained from all fibers for both SL's at 25 and 5°C in the absence of dextran.

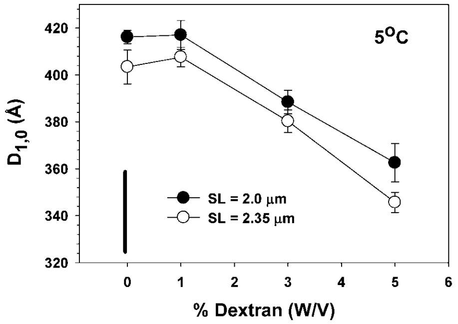

FIGURE 4 Lattice spacing ($D_{1,0}$) was measured at 2.0-μm (●) and 2.35-μm (○) SL in relaxed skinned cardiac trabeculae. Temperature was 5°C. At each SL, lattice spacing was varied independently by osmotic compression with 0–5% dextran T500 in the bathing solutions. Data (means ± SE) were obtained from six preparations. The solid vertical bars in *A* illustrate the change of lattice spacing between 2.0-μm (*top*) and 2.35-μm (*bottom*) SL in intact cardiac trabeculae from rat from Konhilas et al. (2002).

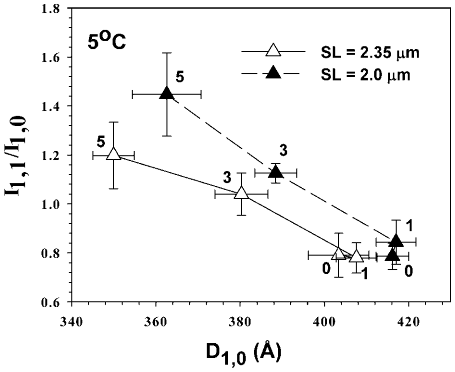

FIGURE 5 The effects of myofilament lattice compression with dextran T500 (% w/v) on the intensity ratio ($I_{1,1}/I_{1,0}$) were determined at 5°C and 170-mM μ. Data (means ± SE) were obtained at 2.0-μm (▲) and 2.35-μm (△) SL from the same fibers as in Fig. 4. The number next to each symbol is the [dextran] (w/v) used to obtain the corresponding $D_{1,0}$ value. The values of $D_{1,0}$ for each [dextran] corresponds to the data in Fig. 4.

At both 25 (Table 1) and 5°C (Fig. 4) $D_{1,0}$ is significantly larger than values reported for intact preparation at either SL (Konhilas et al., 2002). Addition of 5% dextran to bathing solutions restores lattice spacing toward this intact value (Fig. 4). At 5°C decreasing SL caused an increase in $D_{1,0}$ with both zero and 5% dextran ($p < 0.05$), though the reduction of $D_{1,0}$ at 1 and 3% dextran was not significant ($p > 0.05$). The data in Fig. 4 differ somewhat from similar measurements by Konhilas et al. (2002), who observed a much steeper dependence of lattice spacing on SL with zero Dextran than in the presence of dextran. In contrast, we observed roughly parallel changes in $D_{1,0}$ in response to altered SL (Fig. 4); this change was about the same as observed with 3 and 6% dextran by Konhilas et al. (2002). The difference between our results and those of Konhilas et al. (2002) could be related to the 12–20-Å greater lattice spacing they observed; with greater lattice spacing a given change in SL induced a larger change in $D_{1,0}$. In addition to the overall increase in $D_{1,0}$ resulting from skinning of cardiac trabeculae, changing SL between 2.0 and 2.35 μm has a smaller effect on $D_{1,0}$ in the relaxed skinned preparation than in intact trabeculae. Thus to mimic lattice spacing changes that occur in relaxed intact cardiac muscle, osmotic compression of the filament lattice with dextran is necessary in relaxed skinned preparations.

Fig. 5 illustrates that osmotic compression with dextran above 1% significantly ($p < 0.05$) increased the equatorial intensity ratio at 5°C and 170-mM μ at both 2.0-μm (▲) and 2.35-μm (△) SL; 1% dextran did not significantly alter $D_{1,0}$ (Fig. 4) or equatorial intensity ratio (Fig. 5) at either SL. The number next to each symbol is the % dextran (w/v) corresponding to the $D_{1,0}$ value. The values of $D_{1,0}$ for each % dextran corresponds to the data in Fig. 4.

At 5°C the equatorial intensity ratio was lower for a given $D_{1,0}$ value at 2.35- than at 2.0-μm SL (Fig. 5). The difference in equatorial intensity ratio at the two SL's could be explained if at 2.0 μm thick and thin filaments were in full overlap, maximizing the potential for weak Xbr binding, whereas at 2.35 μm overlap, and the relative degree of weak binding, was reduced. The observation that decreasing myofilament overlap causes decreased chord stiffness and weak Xbr binding in skinned skeletal fibers (Brenner et al., 1982) supports this idea. In rat ventricular cardiac muscle thin filament length is ~1 μm (Robinson and Winegrad, 1979) so that at 2.35-μm SL there should be an ~5–10% reduction in the overlap between cardiac thick and thin filaments. This would cause a decrease in the intensity of the 1,1 reflections with no corresponding change in 1,0 intensity.

Effects of SL and osmotic compression with dextran on weak Xbr binding at 5°C

The data in Fig. 5 indicate that at 5°C and 170-mM μ decreasing lattice spacing with Dextran T500 over a range comparable to that occurring during shortening in intact cardiac muscle results in a redistribution of mass toward thin filaments that is consistent with an increase in weak Xbr binding. If this is true increasing $I_{1,1}/I_{1,0}$ ratio should correlate with an increase in chord K under these conditions. For comparison to changes in the $I_{1,1}/I_{1,0}$ equatorial intensity ratio (Fig. 5) corresponding measurements of chord K obtained under the same conditions are illustrated in Fig. 6. Data were obtained at 2.0-μm (*A*) and 2.35-μm (*C*) SL at 5°C and 170-mM μ relaxing solution in the presence (*solid symbols*) and absence (*open symbols*) of 5% dextran. The corresponding difference in stiffness measured at each rate of stretch for individual fibers is illustrated in *C* and *D*, respectively. At 2.0-μm SL passive force and stiffness are low at slow rates of stretch and unaffected by dextran, whereas at faster rates K is elevated by 5% dextran. In contrast at 2.35-μm SL chord K is elevated at all rates of stretch due to substantial passive force and stiffness at that length, as described for Fig. 3. Furthermore, 5% dextran increased K at all rates of stretch, with the enhancement being higher at the faster rates. Thus at both SL's 5% dextran caused an increase in chord K at high rates of stretch that correlates with decreased $D_{1,0}$ (Fig. 4) and increase in $I_{1,1}/I_{1,0}$ (Fig. 5). The increase in chord K with decreased $D_{1,0}$ supports the idea that decreasing lattice spacing increased the probability of weak Xbr binding at 5°C and 170-mM μ.

The data in Figs. 2 and 3 correlate with and support the observations in Fig. 6. Decreasing temperature alone caused an increase in $I_{1,1}/I_{1,0}$ ratio (Fig. 2 *B*) that is accompanied by an increased chord K (Fig. 3) and weak Xbr binding that occurs in the absence of dextran. Fig. 6 indicates that under the same conditions (5°C, 170-mM μ) decreasing $D_{1,0}$ by osmotic compression with 5% dextran lead to further enhancement of chord K. Thus the combination of structural data from x-ray diffraction and mechanical data from

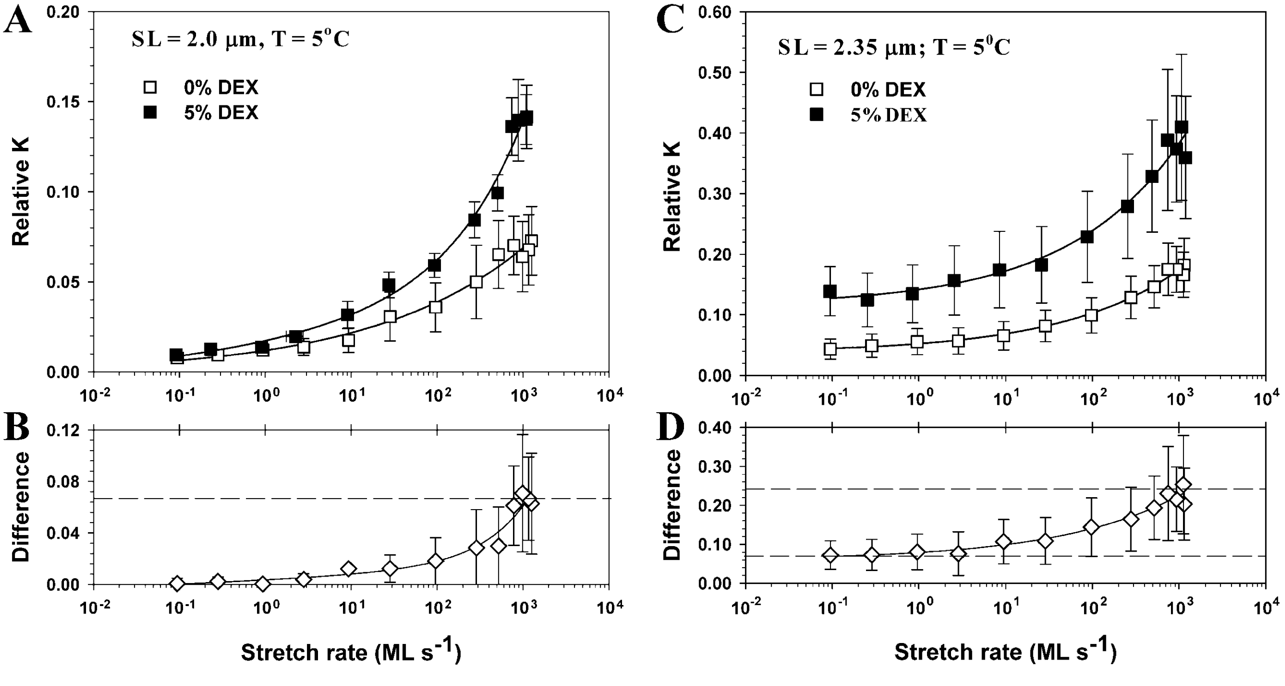

FIGURE 6 For comparison to corresponding changes in the $I_{1,1}/I_{1,0}$ equatorial intensity ratio, chord K was measured at 2.0 (*A*) and 2.35 (*C*) μm at 5°C and 170-mM μ relaxing solution in the presence (*solid symbols*) and absence (*open symbols*) of 5% dextran. The corresponding difference in stiffness measured at each rate of stretch for individual fibers is illustrated in *C* and *D*, respectively. Data were obtained from five to seven preparations. The dotted lines in *B* and *D* are for reference only.

measurements of chord K indicate that the probability of weak Xbr binding is enhanced by decreasing lattice spacing under conditions that favor the population of weak binding Xbr states.

DISCUSSION

These experiments were designed to test the hypothesis that changes in SL and the accompanying changes in myofilament lattice spacing modulate active force generation in cardiac muscle by controlling the probability of Xbr attachment in the initial weak binding states. In resting intact skeletal (Elliott et al., 1967) and cardiac (Matsubara and Millman, 1974) muscle decreasing length causes increased lattice spacing, such that the lattice remains isovolumic. Although corresponding measurements have not been made in cardiac muscle, in skeletal fibers the lattice exhibits isovolumic behavior during contraction (Elliott et al., 1967). Likewise, in intact cardiac muscle the cross-sectional area of central segments increases during active shortening, implying that lattice behavior is also isovolumic during contraction in cardiac muscle (Huntsman et al., 1979, 1983). As a result during diastole increased ventricular filling leads to increased SL and decreased lattice spacing, whereas during the ejection phase of systole decreasing SL is accompanied by increasing lattice spacing. However, whether lattice spacing is an important variable in controlling force has recently been called into question by the observation that force-[Ca^{2+}] relations in skinned cardiac muscle exhibit an SL dependent shift with little change in resting lattice spacing in the presence of low concentrations of dextran T (Konhilas et al., 2002; Moss and Fitzsimons, 2002). But comparison of changes in SL and lattice spacing in relaxed skinned fibers with those occurring during contraction are difficult because Xbr's in either weak or strong binding states exert a radial force (Brenner et al., 1996b; Brenner and Yu, 1991) that decreases lattice spacing in skinned skeletal fibers (Brenner and Yu, 1985). We also found that for trabeculae in rigor lattice spacing was decreased (Table 1), suggesting that strong Xbr binding exerts a radial force on the filament lattice in cardiac muscle, although a previous study reported no difference in lattice spacing between relaxed and rigor conditions in skinned cardiac muscle (Matsubara et al., 1989). In skinned skeletal fibers the radial equilibrium length of active cycling Xbr's is shorter than that of rigor Xbr's (Brenner et al., 1996b), so that lattice spacing could be less than rigor during maximal contraction in skinned cardiac muscle. Resolution of this important issue will have to wait for determination of the relationship between force and lattice spacing in activated skinned cardiac preparations.

The importance that SL dependent changes in lattice spacing play in cardiac force regulation is emphasized by the observations that osmotic compression with dextran T500 caused increased Ca^{2+}-sensitivity of force at short SL's (Fuchs and Smith, 2001; Fuchs and Wang, 1996) and loss of SL effect on force-[Ca^{2+}] relations in skinned cardiac trabeculae (Fuchs and Wang, 1996), and in single skinned cardiac myocytes (McDonald and Moss, 1995) when dextran is used to minimize the difference in lattice spacing between long and short SL's. These considerations, along with the observation that the changes in lattice spacing that accompany SL changes in intact cardiac muscle are much larger than in skinned preparations (Irving et al., 2000) (see Fig. 4), indicate that lattice spacing plays an important role in the regulation of contraction in cardiac muscle.

The influence of SL and lattice spacing on strong and weak Xbr interactions in cardiac muscle

It has been proposed that increasing lattice spacing at short SL results in a decrease in the probability of strong Xbr binding and force generation in skinned skeletal preparations (McDonald et al., 1997). This interpretation was based on the decreased rate of tension redevelopment (k_{TR}) observed in maximally activated fibers at short compared to long SL (McDonald et al., 1997). Thus in cardiac muscle force could be lower at short SL because of a corresponding decreased probability of transition from weak to strong binding Xbr states, a transition that appears to be regulated by Ca^{2+} in skeletal preparations (Brenner, 1986; Regnier et al., 1995). However, this study was in part motivated by our preliminary observations that k_{TR} is unaffected by changes in SL or lattice spacing in skinned skeletal (Moreno Gonzales and Regnier, 2003) and cardiac muscle (Kreutziger et al., 2003) at maximal activation. In skinned cardiac muscle maximal Ca^{2+}-activated force declines 37% when SL is decreased from 2.35 to 2.0 μm, whereas k_{TR} is unaffected (Kreutziger et al., 2003). These preliminary studies indicate that transitions from nonforce to force generating states may be relatively insensitive to changes in SL or lattice spacing at maximal Ca^{2+}-activation in skinned cardiac muscle. If transitions from weak to strong binding Xbr states are not modulated by SL or lattice spacing, the possibility remains that the strong SL and lattice spacing dependence of force, which is the hallmark of the Frank-Starling relationship in cardiac muscle, may result from modulation of weak Xbr binding, as suggested by F. Fuchs (Fuchs and Smith, 2001; Smith and Fuchs, 1999).

We have demonstrated that both lowering temperature (Figs. 2 and 3) and decreased lattice spacing (Figs. 5 and 6) increase weak Xbr binding in relaxed skinned cardiac muscle. Because in skeletal fibers weak Xbr binding has been shown to be obligatory for force generation (Brenner et al., 1996a, 1991; Chalovich et al., 1991), an increased probability of weak Xbr binding in cardiac muscle when lattice spacing is decreased (Figs. 5 and 6) could lead to an increased population of strong binding, force generating Xbr's in the presence of Ca^{2+}. Structural studies indicate that weak attachment results from electrostatic interaction between myosin and the N-terminal domain of actin and are ''non-stereo-specifically'' attached with respect to the actin helix (Xu et al., 1997) and bind with a rapid equilibrium between detachment and attachment in skeletal muscle fibers (Brenner et al., 1984; Kraft et al., 1992; Schoenberg, 1988, 1991). Because chord *K* is elevated only at fast rates of stretch the data in Figs. 3 and 6 suggest that, like skeletal fibers, weak binding in relaxed skinned cardiac muscle is characterized by rapid equilibrium binding.

Comparison of weak Xbr structure in skeletal and cardiac muscle

Lowering temperature has also been shown to favor weak Xbr binding in skinned skeletal fibers (Xu et al., 1997). This was evidenced both by an increase in the equatorial $I_{1,1}/I_{1,0}$ ratio (Xu et al., 1997) and redistribution of Xbr mass from thick to thin filaments at low temperatures and high μ, as well as by disordering of Xbr's relative to the surface of the thick filaments (Malinchik et al., 1997). Subsequent studies suggested that low temperature caused a shift of the population of weak binding Xbr's from the M·ADP·Pi state, which is ordered with respect to the thick filament backbone and less available for weak binding to thin filament sites, to the disordered MgATP state with a higher probability of weak binding (Xu et al., 1999, 2002, 2003). Although our x-ray diffraction patterns from skinned cardiac trabeculae do not have the necessary resolution of on- and off-meridian reflections needed for detailed analysis of Xbr structure, the temperature dependence of changes in the equatorial intensity ratio (Fig. 2 *B*) are similar to skinned skeletal muscle (Xu et al., 1997). Thus, if similar mechanisms are present in skinned cardiac muscle the increase of $I_{1,1}/I_{1,0}$ (Fig. 2 *B*) at low temperature would be consistent with a shift of the weak binding Xbr population from the more ordered M·ADP·Pi to the disordered M·ATP state and increased weak binding, whereas increasing temperature would shift the Xbr population toward the more ordered M·ADP·Pi state and decreased probability of weak Xbr binding.

The correlation of chord *K* and equatorial intensity ratio measurements

Although the distribution and structure of Xbr states can be determined by the measurement of low angle x-ray diffraction, equatorial x-ray measurements alone cannot determine if a corresponding change in the binding of myosin to actin has occurred. Resting stiffness in relaxed fibers suggests the presence of a population of weak binding Xbr's in skeletal fibers in the absence of activating Ca^{2+} (Brenner et al., 1982; Schoenberg, 1988). Resting stiffness increases under conditions such as lowered μ (Brenner et al., 1982) that increase the $I_{1,1}/I_{1,0}$ equatorial intensity ratio in skinned skeletal fibers (Brenner et al., 1984; Xu et al., 1997). Likewise, we found that chord *K* increased when temperature was lowered from 25 to 5°C (Fig. 3), conditions that also resulted in an increase in the $I_{1,1}/I_{1,0}$ ratio (Fig. 2 *B*; Table 1). Thus increasing equatorial intensity ratio at low temperature correlates with an apparent increase in Xbr binding in relaxed cardiac muscle. This suggests, as proposed for skeletal fibers, that lowering temperature caused a shift in the Xbr population toward disordered states with enhanced weak binding to cardiac thin filaments in the absence of Ca^{2+}.

When interfilament spacing ($D_{1,0}$) was decreased with dextran T500 at either 2.0- or 2.35-μm SL both the $I_{1,1}/I_{1,0}$ ratio (Fig. 5) and chord *K* (Fig. 6) increased, particularly at higher rates of stretch. At each SL the range of lattice spacing changes resulting from osmotic compression with 0–5% dextran T500 was nearly the same as observed for intact cardiac trabeculae, although shifted to greater spacing (Fig. 4). The correlation of increasing chord *K* at higher rates of stretch with an increase in the equatorial intensity ratio is consistent with increased weak Xbr binding when interfilament spacing is decreased. The positive correlation of chord *K* and equatorial intensity in Figs. 5 and 6 is similar to that observed when temperature is lowered (Figs. 2 and 3). However, interpretation of the effects of decreasing interfilament spacing with dextran on chord *K* may be complicated by potential effects of dextran itself on Xbr structure. For example, osmotic compression of the myofilament lattice in skinned frog skeletal muscle results in a movement of Xbr mass toward the surface of thick filaments, causing decreased radius of the mass density distribution profile of thick filaments (Irving and Millman, 1989). On the other hand it is not clear how movement of Xbr toward the thick filament surface and away from the thin filaments could by itself lead to an increase in chord *K* at 5°C. Another potential contribution to stiffness measurements might come from the increased viscosity of bathing solutions containing 5% dextran T500. Since skinned cardiac trabeculae are a multicellular preparation, extramyofilament spaces between cells may be accessible to dextran. During rapid length changes movement of viscous fluid between these spaces could occur, creating viscous drag and increased resistance to stretch. Thus stiffness could increase with increased velocity of stretch, even if no changes in weak Xbr binding had occurred. However in addition to increasing chord *K*, 5% dextran caused a significant increase in the $I_{1,1}/I_{1,0}$ ratio (Fig. 5), which is unlikely due to a direct effect of dextran. This together with the positive correlation of changes in chord *K* and equatorial intensity ratio when temperature is lowered in the absence of Dextran (Figs. 2 and 3) is consistent with the proposal that decreasing lattice spacing results in increased weak Xbr binding.

Compared to data obtained at 2.0 μm, at 2.35-μm (Fig. 6, *C* and *D*) SL passive force and stiffness were elevated. Osmotic compression with 5% dextran caused increased chord *K* at all rates of stretch (Fig. 6, *C* and *D*), with the increase being larger at the fastest rates. This result differs from the data in Fig. 3, *C* and *D*, where chord *K* did not increase at low rates of stretch at 2.35-μm SL, when temperature was lowered in the absence of dextran. Although the passive linear stiffness or visco-elastic properties of resting trabeculae resulting from structures other than weak Xbr binding probably did not contribute significantly to the chord *K* results at 2.0-μm SL (Figs. 3, *A* and *B*, and 6, *A* and *B*) because passive force and stiffness were near zero, the same cannot be said of the corresponding results at longer SL. Because of elevated passive tension at 2.35-μm SL mechanical elements of the extracellular matrix, including collagen fibers (Granzier and Irving, 1995), surface cable-like structures on myocytes (Orenstein et al., 1980), as well as intracellular cytoskeletal components, including titin (Granzier and Irving, 1995), all bear load and probably contribute significantly to the chord *K* measurements at the longer length. The complexity of the mechanical contributions of these structures to the stiffness measurements in the presence of resting force at 2.35-μm SL is emphasized by the observation that osmotic compression with 5% dextran caused chord *K* to be elevated at all rates of stretch (Figs. 6, *C* and *D*). This observation implies that compression of the lattice also caused a redistribution of strains within the complex matrix of structures contributing to passive force and stiffness in cardiac muscle. Despite this complexity dextran caused an increase in the difference between chord *K* measurements that was greater at higher rates of stretch at 2.35-μm SL (Fig. 6, *C* and *D*), indicating an increase in weak Xbr binding that correlates with increased equatorial intensity ratio (Fig. 5), as found for shorter SL (Fig. 6, *A* and *B*).

The correlation between decreasing lattice spacing, increasing equatorial intensity ratio (Fig. 5) and increased weak Xbr binding (Fig. 6) at physiologic μ was demonstrated at the unphysiological temperature of 5°C, as these conditions favor weak Xbr attachment (Figs. 2 and 3). This raises the question of whether active force is modulated by SL and lattice spacing effects on weak Xbr binding at more physiological temperatures. At higher temperature one would expect a much smaller, and thus more difficult to detect population of weakly bound Xbr's, as evidenced by the decreased equatorial intensity ratio in skinned cardiac muscle (Fig. 2 *B*; Table 1). However, even though at higher temperatures a smaller fraction of available Xbr's may be weakly bound to thin filaments, their binding is characterized by rapid equilibrium between detachment and attachment. This small population of weak binding Xbr's, the size of which could be altered by SL and lattice spacing, would bind to actin and be continuously and rapidly available for transition into strong binding states in the presence of Ca^{2+}. Thus the data in this study support the previous suggestion (Fuchs and Smith, 2001; Smith and Fuchs, 1999) that the effects of SL and/or lattice spacing on active force generation in cardiac muscle may occur through modulation of the probability of attachment of Xbr's to cardiac thin filaments in the weak binding state.

The authors acknowledge the important contributions made by Mr. Gary Melvin in support of the x-ray measurements at Brookhaven National Laboratories, Lucas Smith and Isaiah Infante, undergraduate assistants with Dr. Martyn, for data analysis, and Anthony Rivera for tissue preparation.

This work was supported by HL67071 (Donald Martyn) and AHA0140040 (Michael Regnier).

REFERENCES

Brenner, B. 1986. The cross-bridge cycle in muscle. Mechanical, biochemical, and structural studies on single skinned rabbit psoas fibers to characterize cross-bridge kinetics in muscle for correlation with the actomyosin-ATPase in solution. *Basic Res. Cardiol.* 81:1–15.

Brenner, B., J. M. Chalovich, L. E. Greene, E. Eisenberg, and M. Schoenberg. 1986. Stiffness of skinned rabbit psoas fibers in MgATP and MgPPi solution. *Biophys. J.* 50:685–691.

Brenner, B., T. Kraft, G. DasGupta, and E. Reisler. 1996a. Cross-bridge binding to actin and force generation in skinned fibers of the rabbit psoas muscle in the presence of antibody fragments against the N-terminus of actin. *Biophys. J.* 70:48–56.

Brenner, B., M. Schoenberg, J. M. Chalovich, L. E. Greene, and E. Eisenberg. 1982. Evidence for cross-bridge attachment in relaxed muscle at low ionic strength. *Proc. Natl. Acad. Sci. USA.* 79:7288–7291.

Brenner, B., S. Xu, J. Chalovich, and L. C. Yu. 1996b. Radial equilibrium lengths of actomyosin cross-bridges in muscle. *Biophys. J.* 71:2751–2758.

Brenner, B., and L. C. Yu. 1985. Equitorial x-ray diffraction from single skinned rabbit psoas fibers at various degrees of activation. *Biophys. J.* 48:829–834.

Brenner, B., and L. C. Yu. 1991. Characterization of radial force and radial stiffness in Ca^{2+}-activated skinned fibres of the rabbit psoas muscle. *J. Physiol. (Lond.).* 441:703–718.

Brenner, B., L. C. Yu, and J. M. Chalovich. 1991. Parallel inhibition of active force and relaxed fiber stiffness in skeletal muscle by caldesmon: implications for the pathway to force generation. *Proc. Natl. Acad. Sci. USA.* 88:5739–5743.

Brenner, B., L. C. Yu, and R. J. Podolsky. 1984. X-ray diffraction evidence for cross-bridge formation in relaxed muscle fibers at various ionic strengths. *Biophys. J.* 46:299–306.

Chalovich, J. M., L. C. Yu, and B. Brenner. 1991. Involvement of weak binding crossbridges in force production in muscle. *J. Muscle Res. Cell Motil.* 12:503–506.

Chase, P. B., D. A. Martyn, and J. D. Hannon. 1994. Activation dependence and kinetics of force and stiffness inhibition by aluminiofluoride, a slowly dissociating analogue of inorganic phosphate, in chemically skinned fibres from rabbit psoas muscle. *J. Muscle Res. Cell Motil.* 15:119–129.

Elliott, G. F., J. Lowy, and B. M. Millman. 1967. Low-angle x-ray diffraction studies of living striated muscle during contraction. *J. Mol. Biol.* 25:31–45.

Fuchs, F. 2002. The Frank-Starling relationship: cellular and molecular mechanisms. *In* Advances in Muscle Research. R. J. Solaro and R. L. Moss, editors. Kluwer, Dordrecht, The Netherlands.

Fuchs, F., and S. H. Smith. 2001. Calcium, cross-bridges, and the Frank-Starling relationship. *News Physiol. Sci.* 16:5–10.

Fuchs, F., and Y.-P. Wang. 1996. Sarcomere length versus interfilament spacing as determinants of cardiac myofilament Ca^{2+} sensitivity and Ca^{2+} binding. *J. Mol. Cell. Cardiol.* 28:1375–1383.

Gordon, A. M., E. Homsher, and M. Regnier. 2000a. Regulation of contraction in striated muscle. *Physiol. Rev.* 80:853–924.

Gordon, A. M., E. Homsher, and M. Regnier. 2000b. Regulation of contraction in striated muscle. *Physiol. Rev.* 80:853–924.

Granzier, H. L., and T. C. Irving. 1995. Passive tension in cardiac muscle: contribution of collagen, titin, microtubules and intermediate filaments. *Biophys. J.* 68:1027–1044.

Head, J. G., M. D. Ritchie, and M. A. Geeves. 1995. Characterization of the equilibrium between blocked and closed states of muscle thin filaments. *Eur. J. Biochem.* 227:694–699.

Huntsman, L. L., D. S. Joseph, M. Y. Oiye, and G. L. Nichols. 1979. Auxotonic contractions in cardiac muscle segments. *Am. J. Physiol.* 237:H131–H138.

Huntsman, L. L., J. F. Rondinone, and D. A. Martyn. 1983. Force-length relations in cardiac muscle segments. *Am. J. Physiol.* 244:H701–H707.

Irving, T. C., J. Konhilas, D. Perry, R. Fischetti, and P. P. de Tombe. 2000. Myofilament lattice spacing as a function of sarcomere length in isolated rat myocardium. *Am. J. Physiol. Heart Circ. Physiol.* 279:H2568–H2573.

Irving, T., and B. Millman. 1989. Changes in thick filament structure during compression of the filament lattice in relaxed frog sartorius muscle. *J. Muscle Res. Cell Motil.* 10:385–396.

Konhilas, J. P., T. Irving, and P. P. de Tombe. 2002. Myofilament calcium sensitivity in skinned rat cardiac trabeculae: role of interfilament spacing. *Circ. Res.* 90:59–65.

Kraft, T., S. Xu, B. Brenner, and L. C. Yu. 1999. The effect of thin filament activation on the attachment of weak binding cross-bridges: a two-dimensional x-ray diffraction study on single muscle fibers. *Biophys. J.* 76:1494–1513.

Kraft, T., L. C. Yu, H. J. Kuhn, and B. Brenner. 1992. Effect of Ca^{2+} on weak cross-bridge interaction with actin in the presence of adenosine 5′-[γ-thio]triphosphate. *Proc. Natl. Acad. Sci. USA.* 89:11362–11366.

Kreutziger, K., A. J. Rivera, D. A. Martyn, and M. Regnier. 2003. Effect of crossbridge kinetics on sarcomere length dependence of force development in cardiac muscle. *Biophys. J.* 84:449a.

Malinchik, S., S. Xu, and L. C. Yu. 1997. Temperature induced structural changes in the myosin thick filament of skinned rabbit psoas muscle. *Biophys. J.* 73:2304–2312.

Malinchik, S., and L. C. Yu. 1995. Analysis of equatorial x-ray patterns from muscle fibers: factors that affect intensities. *Biophys. J.* 68:2023–2031.

Martyn, D. A., and P. B. Chase. 1995. Faster force transient kinetics at submaximal Ca^{2+} activation of skinned psoas fibers from rabbit. *Biophys. J.* 68:235–242.

Matsubara, I., D. W. Maughan, Y. Saeki, and N. Yagi. 1989. Cross-bridge movement in rat cardiac muscle as a function of calcium concentration. *J. Physiol.* 417:555–565.

Matsubara, I., and B. M. Millman. 1974. X-ray diffraction patterns from mammalian heart muscle. *J. Mol. Biol.* 82:527–536.

McDonald, K. S., and R. L. Moss. 1995. Osmotic compression of single cardiac myocytes eliminates the reduction in Ca^{2+} sensitivity of tension at short sarcomere length. *Circ. Res.* 77:199–205.

McDonald, K. S., M. R. Wolff, and R. L. Moss. 1997. Sarcomere length dependence of the rate of tension redevelopment and submaximal tension in rat and rabbit skinned skeletal muscle fibres. *J. Physiol. (Lond.).* 501:607–621.

McKillop, D. F. A., and M. A. Geeves. 1993. Regulation of the interaction between actin and myosin subfragment 1: evidence for three states of the thin filament. *Biophys. J.* 65:693–701.

Moreno Gonzales, A., and M. Regnier. 2003. Effect of crossbridge kinteics on sarcomere length dependence of force development in skeletal muscle. *Biophys. J.* 84:449a.

Moss, R. L., and D. P. Fitzsimons. 2002. Frank-Starling relation: long on importance, short on mechanism. *Circ. Res.* 90:11–13.

Orenstein, J., D. Hogan, and S. Bloom. 1980. Surface cables of cardiac myocytes. *J. Mol. Cell. Cardiol.* 12:771–780.

Regnier, M., C. Morris, and E. Homsher. 1995. Regulation of the cross-bridge transition from a weakly to strongly bound state in skinned rabbit muscle fibers. *Am. J. Physiol.* 269:C1532–C1539.

Robinson, T. F., and S. Winegrad. 1979. The measurement and dynamic implications of thin filament lengths in heart muscle. *J. Physiol.* 286:607–619.

Schoenberg, M. 1985. Equilibrium muscle cross-bridge behavior: theoretical considerations. *Biophys. J.* 48:467–475.

Schoenberg, M. 1988. Characterization of the myosin adenosine triphosphate (M.ATP) crossbridge in rabbit and frog skeletal muscle fibers. *Biophys. J.* 54:135–148.

Schoenberg, M. 1991. Effect of ionic strength on skinned rabbit psoas fibers in the presence of magnesium pyrophosphate. *Biophys. J.* 60:690–696.

Schoenberg, M., B. Brenner, J. M. Chalovich, L. E. Greene, and E. Eisenberg. 1988. Cross-bridge attachment in relaxed muscle. *Adv. Exp. Med. Biol.* 170:269–284.

Smith, S. H., and F. Fuchs. 1999. Effect of ionic strength on length-dependent Ca^{2+} activtion in skinned cardiac muscle. *J. Mol. Cell. Cardiol.* 31:2115–2125.

Squire, J. 1981. The Structural Basis of Muscular Contraction. Plenum Publishers, New York.

Xu, S., J. Gu, T. Rhodes, B. Belknap, G. Rosenbaum, G. Offer, G. White, and L. C. Yu. 1999. The M.ADP. Pi state is required for helical order in the thick filaments of skeletal muscle. *Biophys. J.* 77:2665–2676.

Xu, S., S. Malinchik, D. Gilroy, T. Kraft, B. Brenner, and L. C. Yu. 1997. X-ray diffraction studies of cross-bridges weakly bound to actin in relaxed skinned fibers of rabbit psoas muscle. *Biophys. J.* 73:2292–2303.

Xu, S., J. Gu, G. Melvin, and L. C. Yu. 2002. Structural characterization of weakly attached cross-bridges in the A.M.ATP state in permeabilized rabbit psoas fibers. *Biophys. J.* 82:2111–2122.

Xu, S, G. Offer, J. Gu, H. White and L. C. Yu. 2003. Temperature and ligand dependence of conformation and helical order in myosin filaments. *Biochemistry.* 42:390–401.

Yu, L. 1989. Analysis of equitorial x-ray diffraction patterns from skeletal muscle. *Biophys. J.* 55:433–440.

Yu, L. C., A. C. Steven, G. R. S. Naylor, R. C. Gamble, and R. J. Podolsky. 1985. Distribution of mass in relaxed frog skeletal muscle and its redistribution upon activation. *Biophys. J.* 47:311–321.